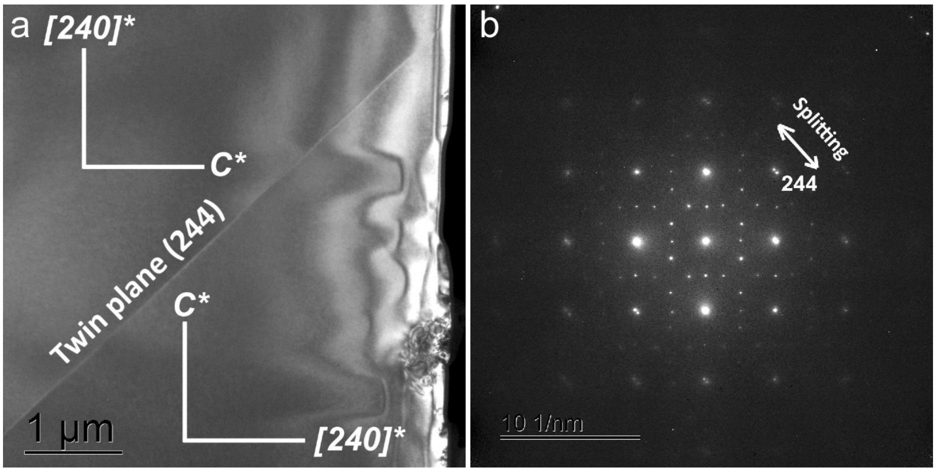

Fig. 3.3-9: (a) Dark-field TEM image (with **g** = 244) of a twinned wadsleyite grain. (b) SAED pattern of the [210] zone axis from an area including the composition plane.

j. *A new evaluation method of cation ordering history in eclogite-facies omphacite (R. Fukushima and T. Tsujimori/Sendai, N. Miyajima)*

Low-temperature eclogite, which commonly occurs in Phanerozoic subduction-related orogens, has received considerable attention because of its crucial role as a natural laboratory for subduction-zone geodynamics. Notably, omphacite ($\sim Ca_{0.5}Na_{0.5}[Mg,Fe^{2+}]_{0.5}Al_{0.5}Si_2O_6$), an index mineral of eclogite facies, has the potential to reveal kinetics of eclogitisation of subducted oceanic crust. For example, growth and coarsening of antiphase domains (APDs) – a disequilibrium microstructure reflecting a higher-order phase transformation from cation-disordered (*C*2/*c*) to cation-ordered (*P*2/*n*) states – occurs within blueschist- to eclogite-facies omphacites (Fig. 3.3-10a,d). Therefore, detailed analysis of APD textures, even for each omphacite grain, enables a discussion of its temperature-time (*T*-*t*) history.

Thus far, geoscientists have struggled to utilise disequilibrium textures in metamorphic minerals to unravel past geological processes. Reconnaissance of APD textures in omphacite has proved to be challenging for obtaining a specific snapshot of its time evolution. Based on the classical APD-coarsening law in alloys and size dependence on annealing time and temperature, pioneering work in the literature proposed a geospeedometer using the mean size of equiaxed APDs in omphacite. Nevertheless, a question arises whether the parameter 'mean APD size' is truly appropriate to evaluate various metamorphic *T*–*t* paths in general. This is because variations in chemical composition and density of vacancies in natural omphacites might affect individual nucleation/growth rates of initially ordered domains.

To tackle this problem, we extracted multiple characteristic values from dark-field transmission electron microscope (TEM) images of omphacite in epidote eclogites from two different localities: Syros (Greece) and Omi (Japan). With digital image processing, we obtained four parameters for each: 1) mean APD size: δ (manually measured along 200 × 200 nm^2 grids); 2) area proportion of the ordered phase: *F* (Fig. 3.3-10b,e); 3) spatial wavelength calculated from

2-dimensional autocorrelation: λ (Fig. 3.3-10b,e); and 4) spatial density of antiphase domain boundaries: L (Fig. 3.3-10c,f). Because λ and L values are respectively related to representative distances of adjacent ordered domains and their spatial density, these parameters could reveal nanotextural changes in the APD nucleation-growth regime. Despite the different magnifications and resolutions of the two images, our results clearly demonstrate that ordered domains in the Syros omphacite are smaller and more sparsely distributed in the disordered matrix. We can interpret the cause as either annealing time difference, temperature difference, or compositional difference that regulates the initial stage of APD appearance. This result suggests that natural omphacite can be incompletely ordered, which would imply that simple application of the coarsening rate law is prohibited. Our method for post hoc analysis of equiaxed APD textures provides a new way to investigate APD growth/coarsening kinetics in omphacite, which has previously not been possible using only mean APD sizes.

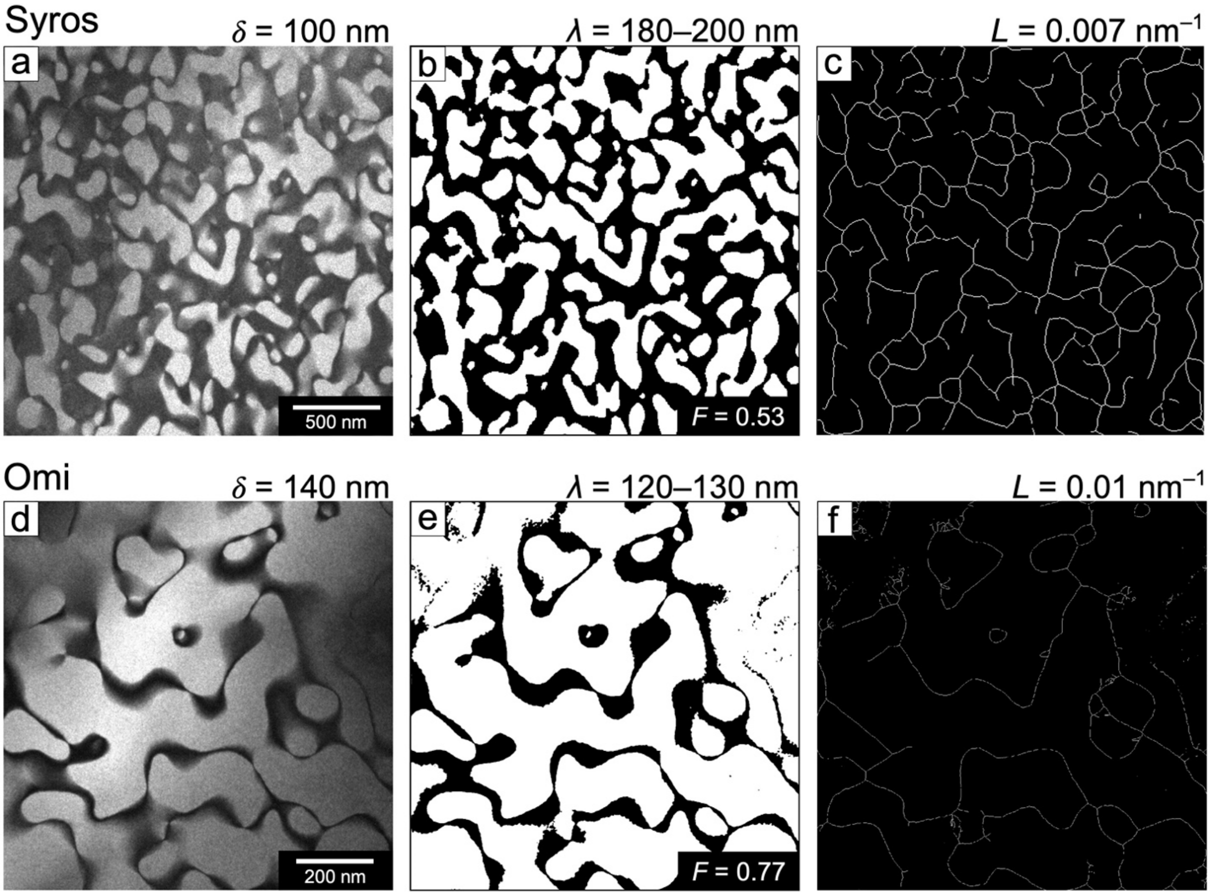

Fig. 3.3-10: Examples of acquired/processed TEM images of natural omphacites from Syros (a-c) and Omi (d-f). (a) dark-field TEM image with g = 050 showing equiaxed APDs (δ = 100 nm); (b) binarised image with black/white regions as disordered/ordered domains, respectively (F = 0.53, λ = 180-200 nm); (c) antiphase domain boundaries (1-pixel width) extracted from the binarised image (L = 0.007 nm^{-1}); (d) dark-field image with g = 050; δ = 140 nm; (e) binarised image (F = 0.77, λ = 120-130 nm); (f) antiphase domain boundaries (L = 0.01 nm^{-1}). Note that the two TEM images (a and d) are different in magnification and resolution. Image processing was performed with MATLAB scripts.